Panoramic Bundle Block Adjustment with Image Matching for Mobile Mapping System

Uthaisri, P.,[1,2]* Santitamnont, P.[1] and Mityodwong, T.[1]
[1]Department of Survey Engineering, Faculty of Engineering, Chulalongkorn University, Bangkok 10330 Thailand; E-mail:puthaisri@gmail.com*, phisan.chula@gmail.com, tanaratm@gmail.com
[2]Department of Civil Engineering and Environmental Engineering, Faculty of Engineering, Rajamangala University of Technology Lanna, Chiangmai 50300
Correspondence Author

Abstract
The spherical panoramic image from Ladybug3 in MMS can determine the coordinate of ground point without data from INS. The new mathematical model for spherical panoramic image and new procedure for image matching were developed for bundle block adjustment. Comparing result between data from INS and bundle block adjustment based on 20 check points. The RMSE will check in X, Y and Z direction. The reference result is determined from INS data the RMSE are±0.216 m., ±0.362 m. and ±0.308 m. respectively. However, when the manual tie points and photo control points added in first and last image are used, the corresponding RMSE are ±0.085 m., ±0.100 m. and ±0.039 m. respectively. When applied photo control points to all images the RMSE are ±0.092 m., ±0.109 m. and ±0.041 m. respectively. In addition, using tie points from computer vision and control points produce are ±0.303 m., ±0.330 m. and ±0.202 m. Finally, the RMSE decrease respectively to ±0.128 m., ±0.230 m. and ±0.071 m. after control points are added to all images

1. Introduction

The mobile mapping system (MMS) has now become popular in modern surveying and GIS. The panoramic image from MMS has advantages over a normal image[1]. While taking images, an Inertial Measurement System (INS) in MMS can acquire image exterior orientation parameters or EOP, that is, the location from the Global Navigation Satellite System (GNSS) and the orientation of the camera platform and vehicle from the Inertial Measuring Unit (IMU). The EOP are important and may be used to compute coordinates of the point of interest in an image. The classic problem in working with MMS in an urban area is the blocking of a GNSS signal by high rise buildings. Although an IMU can recover a lost signal, it has some limitations: the error will increase with time when vehicle moves slowly or stops completely (Grejner-bzezlnska et al., 2005). The collinearity equation in photogrammetry, the relationship between ground points, image points, and projective center, can compute image exterior orientation parameters via a resection method (Santitamnont, 2012). Bundle block adjustment is a popular method to adjust the colinearity equation for estimating image exterior orientation parameters (Tae-Wan and Im-Pyeong, 2010 and Uthaisri et al., 2014). Feature detection and matching by computer vision can detect interest points on an image and match them with two or more images (Szeliski, 2011). It is a great chance to use it to find tie point for bundle block adjustment. This research will demonstrate a method for using automatic tie points in computer vision and compare the results of coordinates of point of interest using exterior orientation parameters obtained from the MMS and the bundle block adjustment.

2. Literature Review

The first MMS was studied and developed between the 1980s and the 1990s at Ohio State University by the Center for Mapping under the GPSVan project (Novak and Bossler 1995 and Bossler and Toth, 1996). At the same time the VISAT system was developed in University of Calgary in 1993 for the mapping of highway corridor information (El-Sheimy and Schwarz, 1993). After that, the MMS steadily developed. The system consists of a vehicle (platform) and sensors. A vehicle can be a car, a train, a boat, an aircraft or even a human being. Sensors can be divided into Navigation sensors and Mapping sensors.

[1]Normal image is image take from normal lens (usually 50 mm.) in 35 mm. film format

Ellum and El-Sheimy, (2002) had gathered data, determining the location of the vehicle when, until 2002, all MMS used GPS as the primary location sensor. Additional equipment such as IMU, Gyrometer, Inclinometer, Odometer are now used to fine-tune location or help determine location in a lost GPS signal area. A Mapping sensor can be a still camera, a motion camera or a video camera. There are also single-cameras and multi-cameras, analog and digital. Nowadays, the new global positioning system, GNSS, plays an active role and is slowly replacing GPS. Modern digital cameras, both single and multi-camera, have been used in the study to provide not only single images but also panoramic images from a multi-camera. A spherical panoramic image can be used to determine coordinates for point of interest in photogrammetry. It can compute coordinates of point if that point appears on two or more images. Image recognition is accomplished by pairing similar images which define the point of interest by using an optimized processing technique such as FAST (Features from Accelerated Segment Test), which is an algorithm for identifying interest points in an image. The circle with a 16-pixel perimeter from the center is a test point with the contrast of greyscale color around perimeter. The test pixel will be a corner or interest point if that pixel is brighter or darker than the test point in at least three directions (Edward and Drummond , 2006).As FAST can only find interest points when all interest points have been selected in one image, a different process is necessary to find the individual character of each point to use in image matching for other images. The SIFT (Scale Invariant Feature Transform) is an algorithm used to find interest points, called keypoints, and information around keypoints that is called a descriptor in image. Indeed, SIFT is named after the method of transforming image data to coordinate system that is invariant to image scaling, translation, and rotation with local features. One can use SIFT to start searching for interest points by convolving an image with a Gaussian filter in difference scales. Key locations are defined as the maxima and minima of the result of the 'difference of Gaussians (DOG)' function applied in 'scale space' to a series of smooth and resampling images. Dominant orientations are assigned to localized keypoints. Each keypoint is assigned one or more orientations in difference scale to determine magnitude and direction. This ensures invariance to image location, scale and rotation. The keypoint descriptor is a vector that has128 elements. It calculates from histograms around a keypoint. These histograms are computed from magnitude and orientation values of samples around the keypoint (Lowe, 1999). Another technique is SURF (Speeded Up Robust Features), an algorithm similar to SIFT for determining points of interest. SURF was developed by Herbert et al., 2006 to increase processing efficiency. Its main principle is finding a keypoint, computing by integral image and convolution with an estimation of Gaussian second derivative instead of Gaussian Filters. This method greatly reduces computing time. A Hessian matrix-base is used to determine which point is the point of interest and to define the location of that point of interest on the image. The distinctive character of the point of interest is determined by segmenting the area surrounding point of interest into sub-regions of 4 x 4. Each segment is computed using the Harr wavelet along both the x and y- axes, weighted by the Gaussian Kernel to determine the interest point orientation. A vector representing a point of interest can be classified from each sub-region having a four dimensional descriptor vector. Having compared all three techniques, SIFT, SURF and FAST, Maridalia Guerrero Pena concluded that FAST gives more points of interest but cannot identify distinctive character on an image, FAST also does best in manually finding image matching but it cannot perform the task automatically. However, SIFT gives better image matching than SURF but it is more time consuming to use (Guerrero, 2011). In Figure 1 show the sample of panoramic image was detected keypoints by FAST, SIFT, and SURF. With the 5400x2700 pixel size panoramic image FAST detected 48898 keypoints in 0.056 second SIFT detected 22763 keypoints in 7.412 seconds and 15.217 seconds with point descriptor the last one SURF detected 36039 keypoints in 2.699 seconds and 7.701 seconds with point descriptor. Image matching using distinctive character of point of interest can likewise by conducted with FLANN (Fast Library for Approximate Nearest Neighbors), a library for performing fast approximate nearest neighbor searches. We can find a point in P, nearest to Q, given a set of points P in a matric space X but these points must be preprocessed in such a way as to yield a new query point $Q \in X$ (Muja and Lowe, 2013).

3. Methodology

3.1 Mathematical Model for Spherical Panoramic Image

The coordinates of a spherical panoramic image are computed on the basis of Aerial Photogrammetry using Bundle Block Adjustment from a perspective image. With a mathematical model for spherical panoramic image, the resultant image from Ladybug3 is projected in an equi-rectangular way and, hence, angular reference coordinates can be

located on the image using Fangi's concept from Spherical Photogrammetry (Fangi, 2007). As shown in Figure 2. We use a collinearity equation to explain the relationship between points on an image and on the ground (Figure 3). It can be seen that the beam vector from projector 'O' through the spherical plane point a to A on the ground is linear. Figure 3 is a spherical panoramic image and any point on it can be measured by its horizon angle (μ) and zenith angle (υ).

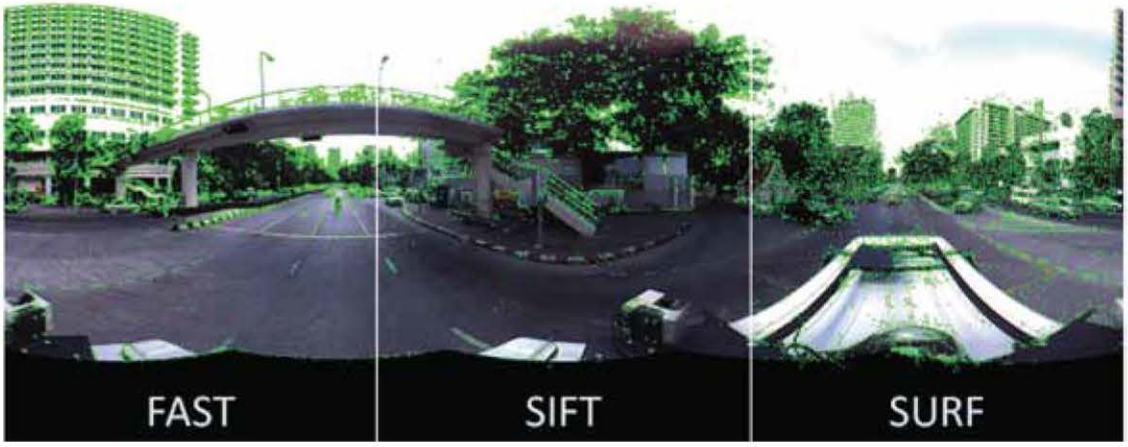

Figure 1: Sample panoramic image with keypoints by FAST, SIFT and SURF.

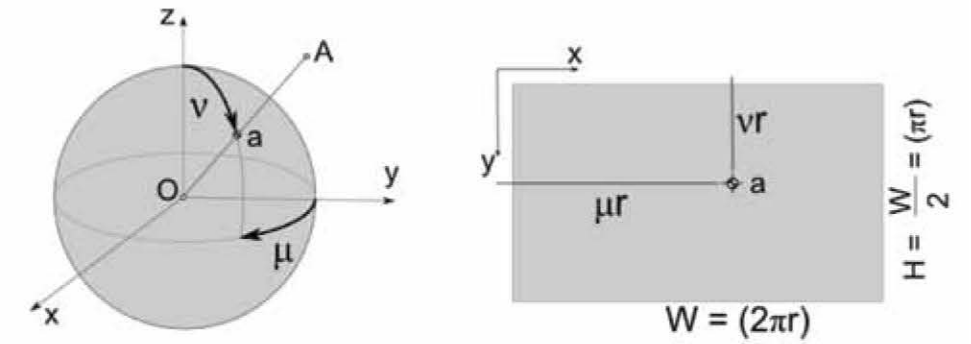

Figure 2: Polar coordinate and image coordinate.

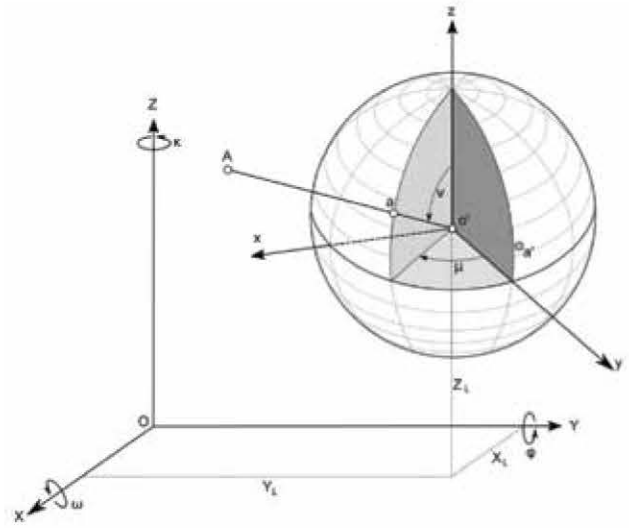

Figure 3: Relationship between object coordinate and spherical coordinate

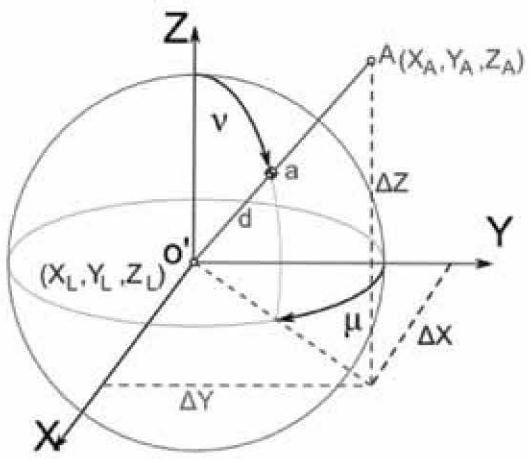

Figure 4: Relationship between polar coordinate and rectangular coordinate

Reference coordinates of point A on the ground are transferred to point a on the spherical image using a rectangular coordinate system and a polar coordinate system (Figure 4). We can find coordinates of point A in relation to the spherical center as follows:

$$\begin{bmatrix} \Delta X \\ \Delta Y \\ \Delta Z \end{bmatrix} = \begin{bmatrix} X_A - X_L \\ Y_A - Y_L \\ Z_A - Z_L \end{bmatrix}$$ Equation 1

The coordinates of point a can be computed thus:

$$\mu = \tan^{-1}(\Delta X / \Delta Y)$$ Equation 2

$$v = \cos^{-1}\frac{\Delta Z}{d}$$ Equation 3

$$d = \sqrt{\Delta X^2 + \Delta Y^2 + \Delta Z^2}$$ Equation 4

Together with an angle around the X Y and Z axes, the coordinates of point a in relation to the spherical center can be computed as:

$$\begin{bmatrix} \Delta x' \\ \Delta y' \\ \Delta z' \end{bmatrix} = \begin{bmatrix} R_{11} & R_{12} & R_{13} \\ R_{21} & R_{22} & R_{23} \\ R_{31} & R_{32} & R_{33} \end{bmatrix} \begin{bmatrix} \Delta X \\ \Delta Y \\ \Delta Z \end{bmatrix}$$ Equation 5

The values of μ and υ can be solved according to the equations below:

$$\mu = \tan^{-1}\frac{\Delta x'}{\Delta y'}$$ Equation 6

$$v = \cos^{-1}\frac{\Delta z'}{d}$$ Equation 7

$$\mu = \tan^{-1}\frac{R_{11}\Delta X + R_{12}\Delta Y + R_{13}\Delta Z}{R_{21}\Delta X + R_{22}\Delta Y + R_{23}\Delta Z}$$ Equation 8

$$v = \cos^{-1}\frac{R_{31}\Delta X + R_{32}\Delta Y + R_{33}\Delta Z}{\sqrt{\Delta X^2 + \Delta Y^2 + \Delta Z^2}}$$ Equation 9

Where the rotation matrix is:

$R_{11} = \cos\varphi\cos\kappa + \sin\varphi\sin\omega\sin\kappa$
$R_{12} = -\cos\varphi\sin\kappa + \sin\varphi\sin\omega\cos\kappa$
$R_{13} = \sin\varphi\cos\omega$
$R_{21} = \cos\omega\sin\kappa$
$R_{22} = \cos\omega\cos\kappa$
$R_{23} = -\sin\omega$
$R_{31} = -\sin\varphi\cos\kappa + \cos\varphi\sin\omega\sin\kappa$
$R_{32} = \sin\varphi\sin\kappa + \cos\varphi\sin\omega\cos\kappa$
$R_{33} = \cos\varphi\cos\omega$

3.2 Panoramic Image Matching

Panoramic image matching by computer vision begins with finding a point of interest and its distinctive character using SURF technique which gives a faster result than SIFT for panoramic image size of 5400x2700 pixels, segmenting only the region of interest (Figure 5) by using mask (Figure 6) in order to exclude the overlapping area between image and vehicle.

Figure 5: Area of interest in panoramic from Ladybug3

Figure 6: Mask

Then FLANN is used to perform image matching. After that, the result is filtered by area zone, and finally subjected to a radius filter to reduce its number of points. The process flow chart is shown in Figure 7. To match two images, we start with a search for a keypoint and a description in each image by using SURF technique with mask. Then image matching is based on point description by FLANN method. The result may contain numerous point pairs but also mismatched points. With mask the area of interest will be divided into 5 zones.

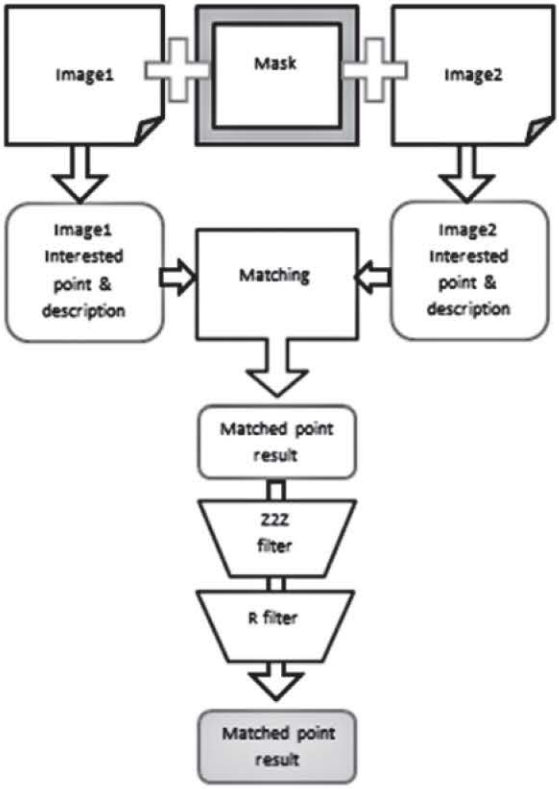

Figure 7: Image matching diagram

Using Zone to Zone filer (Z2Z filter) will eliminate the cross zone matching points. In the end, the matches will be reduced from more than 10,000 points to about 40-50 points which can be visually checked. The R filter in the diagram is the radius filter. The first random point will set to the first center. Match points in the circle area around the first point will be eliminated. Then we locate the next random point and repeat the process until the distance between match points exceeds the setting radius.

In this research we use 200 pixels of radius to reduce match points to 40-50 points. Match points are distributed over 5 zones.

3.3 Panoramic Bundle Block Adjustment

The coordinates of an object are determined from spherical panoramic image according to the principle of having an object appear on one or more images using the intersection of ray vectors from perspective center to point A. Figure 8 show example image intersection from 2 panoramic images. From Figure 8, the EOP of spherical images 1 and 2 areO_1 ($X0_1$, $Y0_1$, $Z0_1$,ω_1,φ_1,κ_1) andO_2 ($X0_2$, $Y0_2$, $Z0_2$,ω_2,φ_2,κ_2) respectively. For an object, A, its coordinates on panoramic image can be measured as a_1 (μ_1,v_1) for image 1 and a_2 (μ_2,v_2) for image 2 using the relationship of collinearity equation of spherical panoramic image as follows:

$$\mu_{a_1} = \tan^{-1}\frac{R_{11}^{[1]}\Delta X^{[1]} + R_{12}^{[1]}\Delta Y^{[1]} + R_{13}^{[1]}\Delta Z^{[1]}}{R_{21}^{[1]}\Delta X^{[1]} + R_{22}^{[1]}\Delta Y^{[1]} + R_{23}^{[1]}\Delta Z^{[1]}}$$

Equation 10

$$v_{a_1} = \cos^{-1}\frac{R_{31}^{[1]}\Delta X^{[1]} + R_{32}^{[1]}\Delta Y^{[1]} + R_{33}^{[1]}\Delta Z^{[1]}}{\sqrt{\Delta X^{[1]2} + \Delta Y^{[1]2} + \Delta Z^{[1]2}}}$$

Equation 11

$$\mu_{a_2} = \tan^{-1}\frac{R_{11}^{[2]}\Delta X^{[2]} + R_{12}^{[2]}\Delta Y^{[2]} + R_{13}^{[2]}\Delta Z^{[2]}}{R_{21}^{[2]}\Delta X^{[2]} + R_{22}^{[2]}\Delta Y^{[2]} + R_{23}^{[2]}\Delta Z^{[2]}}$$

Equation 12

$$v_{a_2} = \cos^{-1}\frac{R_{31}^{[2]}\Delta X^{[2]} + R_{32}^{[2]}\Delta Y^{[2]} + R_{33}^{[2]}\Delta Z^{[2]}}{\sqrt{\Delta X^{[2]2} + \Delta Y^{[2]2} + \Delta Z^{[2]2}}}$$

Equation 13

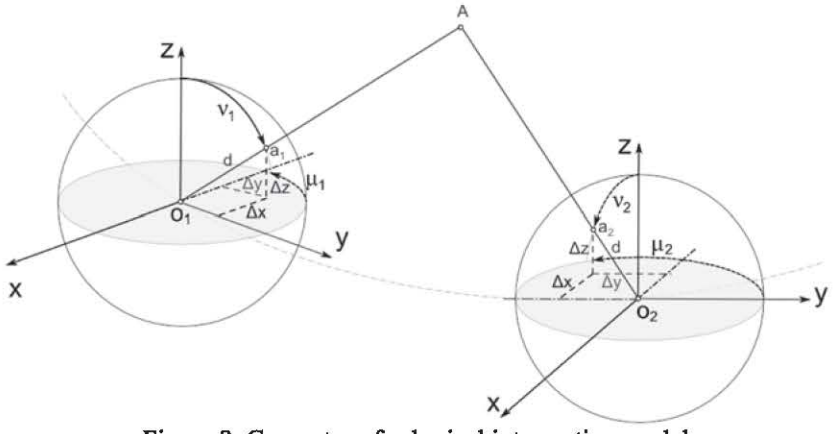

Figure 8: Geometry of spherical intersection model

The product of least square equation technique is computed where the is a function of colinearity equation of spherical panoramic image is:

$$F_1 = \mu_{a_1} - \tan^{-1}\frac{R_{11}^{[1]}\Delta X^{[1]} + R_{12}^{[1]}\Delta Y^{[1]} + R_{13}^{[1]}\Delta Z^{[1]}}{R_{21}^{[1]}\Delta X^{[1]} + R_{22}^{[1]}\Delta Y^{[1]} + R_{23}^{[1]}\Delta Z^{[1]}}$$

$$F_2 = \nu_{a_1} - \cos^{-1}\frac{R_{31}^{[1]}\Delta X^{[1]} + R_{32}^{[1]}\Delta Y^{[1]} + R_{33}^{[1]}\Delta Z^{[1]}}{\sqrt{\Delta X^{[1]^2} + \Delta Y^{[1]^2} + \Delta Z^{[1]^2}}}$$

$$F_3 = \mu_{a_2} - \tan^{-1}\frac{R_{11}^{[2]}\Delta X^{[2]} + R_{12}^{[2]}\Delta Y^{[2]} + R_{13}^{[2]}\Delta Z^{[2]}}{R_{21}^{[2]}\Delta X^{[2]} + R_{22}^{[2]}\Delta Y^{[2]} + R_{23}^{[2]}\Delta Z^{[2]}}$$

$$F_4 = \nu_{a_2} - \cos^{-1}\frac{R_{31}^{[2]}\Delta X^{[2]} + R_{32}^{[2]}\Delta Y^{[2]} + R_{33}^{[2]}\Delta Z^{[2]}}{\sqrt{\Delta X^{[2]^2} + \Delta Y^{[2]^2} + \Delta Z^{[2]^2}}}$$

Equation 14

Then, by substituting (X_A, Y_A, Z_A) with the approximated value, $\mathbf{x} = (X_A^0, Y_A^0, Z_A^0)$, the value of matrix f can be computed as thus:

$$\mathbf{f} = \begin{bmatrix} F_1 \\ F_2 \\ F_3 \\ F_4 \end{bmatrix}$$

Equation 15

Matrix B is found by the derivatives of function f with respect to an unknown (X_A, Y_A ,Z_A)

$$\mathbf{B} = \begin{bmatrix} \frac{\partial F_1}{\partial X_A} & \frac{\partial F_1}{\partial Y_A} & \frac{\partial F_1}{\partial Z_A} \\ \frac{\partial F_2}{\partial X_A} & \frac{\partial F_2}{\partial Y_A} & \frac{\partial F_2}{\partial Z_A} \\ \frac{\partial F_3}{\partial X_A} & \frac{\partial F_3}{\partial Y_A} & \frac{\partial F_3}{\partial Z_A} \\ \frac{\partial F_4}{\partial X_A} & \frac{\partial F_4}{\partial Y_A} & \frac{\partial F_4}{\partial Z_A} \end{bmatrix}$$

Equation 16

The result can be computed and adjusted by:

$$\Delta^0 = \mathbf{N}^{-1}\mathbf{t}$$

Equation 17

Where

$\mathbf{N} = \mathbf{B}^T\mathbf{W}\mathbf{B}$

$t = \mathbf{B}^T\mathbf{W}\mathbf{f}$

$\mathbf{W}$ = weight matrix

If the solution is greater than the accuracy of the defined result, then that result should be added to the first estimation values as iteration is performed.

$$\mathbf{x}_{new} = \mathbf{x} + \Delta^0$$

Equation 18

Continue the iteration until $\Delta \leq \varepsilon$

3.4 Data Acquisition

The test area shown in Figure 9 is located on Henry Dunant road, near Chulalongkorn University, Bangkok, Thailand. The data was recorded by the MMS vehicle with image sensors and location sensors. The MMS instrument contains Ladybug3, the omni-directional camera, SICK, the laser scanner for image sensors, and INS for the location sensors. INS uses GPS IMU and the distance measuring instrument (DMI) to compute the location of the vehicle and instruments. This paper uses only spherical panoramic image size of 5400x2700 pixels from Ladybug3 and location data from the INS. The panoramic image will be extracted from Ladybug3 by using Ladybug SDK software. The trajectory file contains the location and orientation of Ladybug3 offset from INS. The location and orientation used to be the EOP of each image. There are 50 control points with known coordinates that were established by a ground survey using GPS and Total station for ground control points and check points (Figure 10). Figure 11 show example panoramic image show ground control points.

There are 5 test cases:

Case 1: uses EOP from INS to find point coordinates.

Case 2: uses EOP from Bundle block adjustment using ground control point on first and last images with manual tie points to find point coordinates.

Case 3: uses EOP from Bundle block adjustment using control point on all images with manual tie points to find point coordinates.

Case 4: uses EOP from Bundle block adjustment using control points on first and last images with tie points from computer vision method.

Case 5: uses EOP from Bundle block adjustment using control points on all images with tie points from computer vision method.

Ground control points and tie points on image in each case are shown in Figure 12.

Figure 9: Test site on Henry Dunant road, Thailand

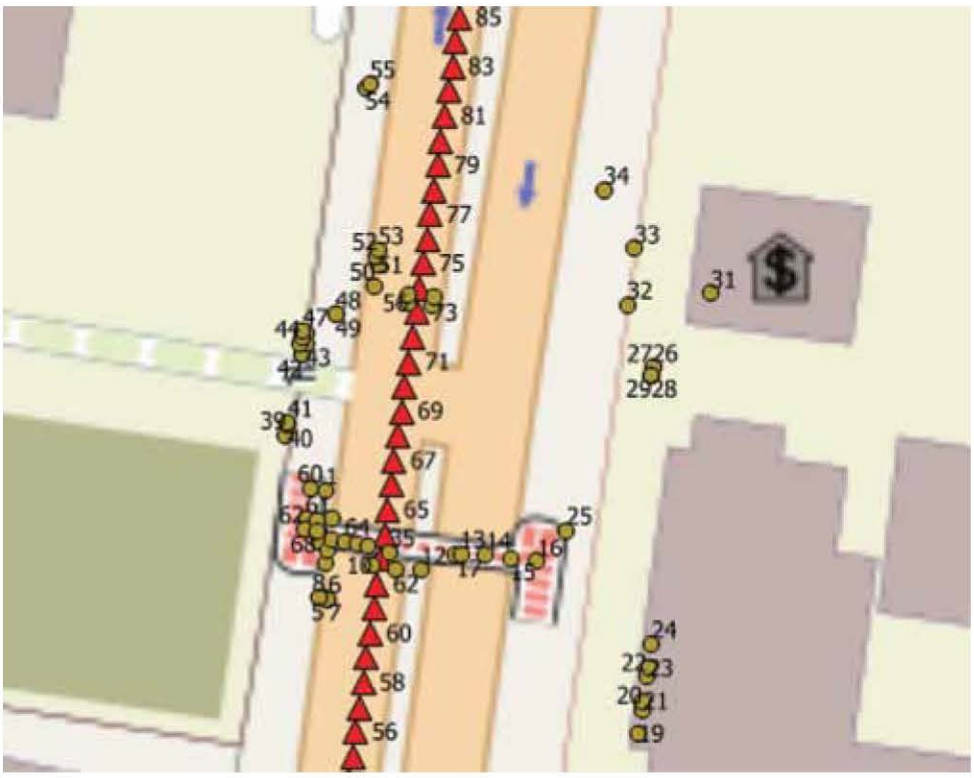

Figure 10: Control points on map (circle with number)

Figure 11: Sample image with control points

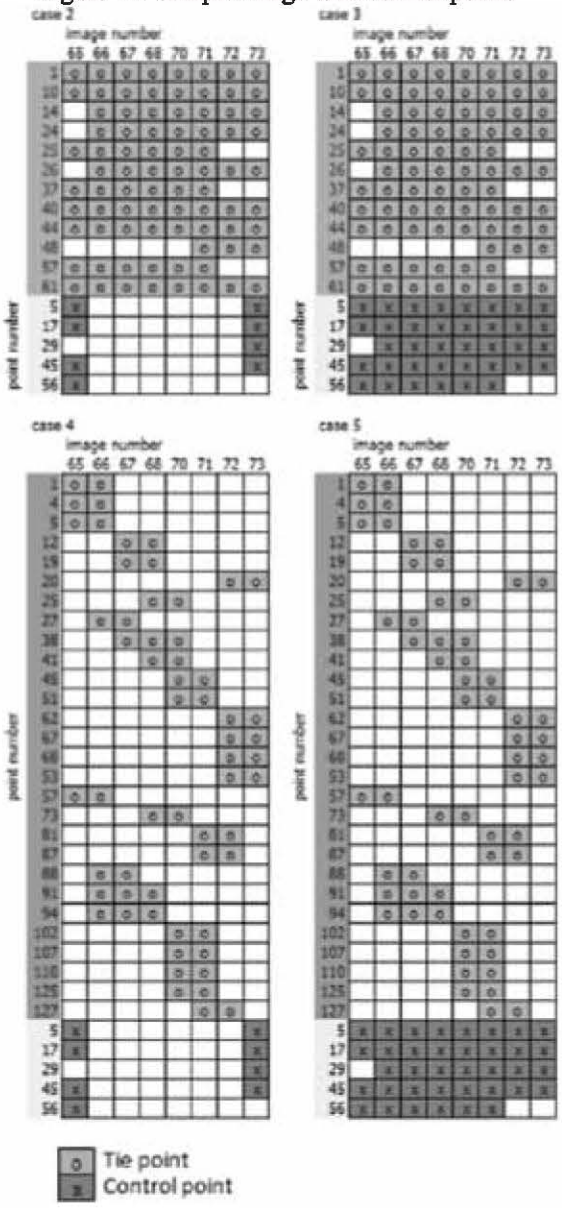

Figure 12.Tie points and ground control points on image

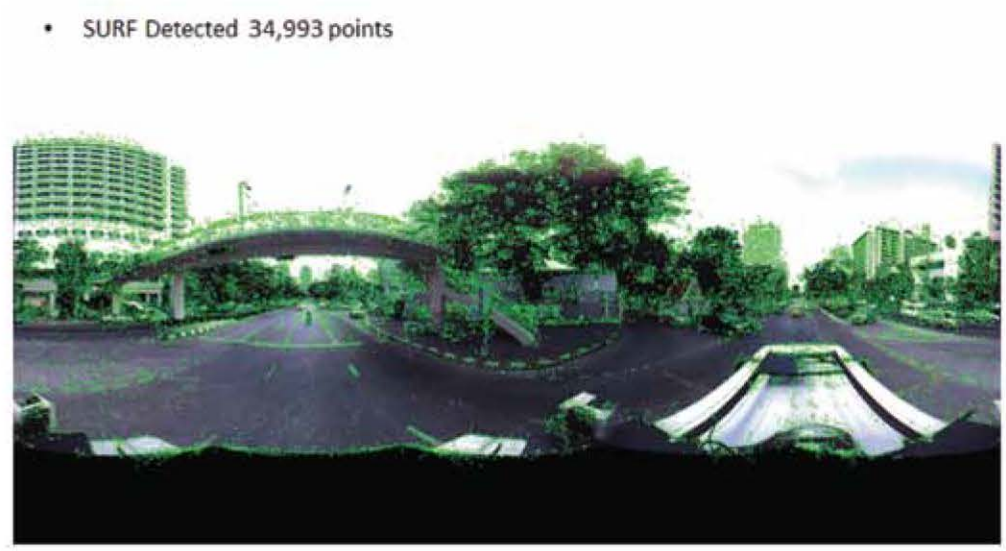

Figure 13: Interest points by SURF

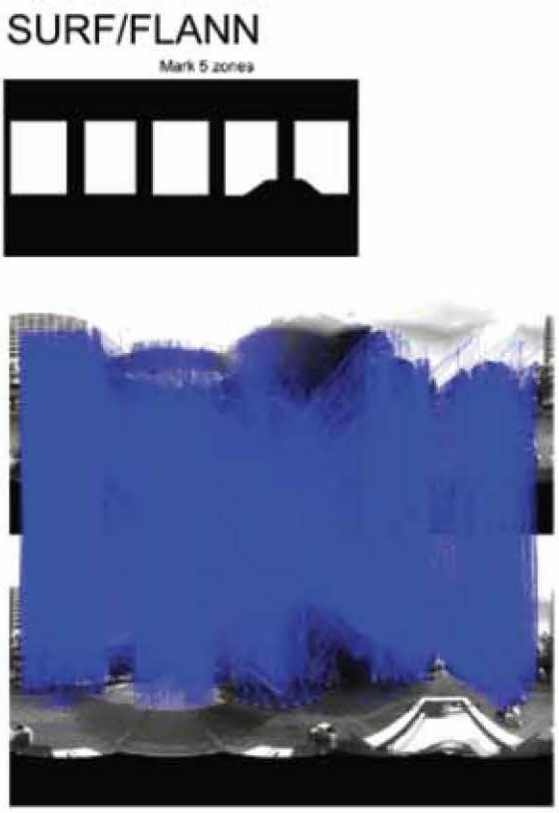

Figure 14: FLANN Matched result

4. Results and Discussion

4.1 Image Matching Result

The result of interest points on image using the SURF method is shown in Figure 13. When image matching is performed with a subsequent image using FLANN, the result is shown in Figure 14 matched points appear only in a masking zone. The 20713 matched points found in different zones are considered mismatches. After Zone-to-zone filter is applied, the sample result is shown in Figure 15. The matched points are located same zone number in each image. The matched points reduce to 11279 points on sample image. According to collinearity equations and the mathematical model, a minimum of 3 points was found on an image. More points, however, will make the model stronger and minimize mismatches. The number of matched points will be reduced to 30-50 points by Radius Filter. Figure 16 shows the sample result of Radius filter using R = 200 pixels. The 56 matched points found.

4.2 Bundle Block Adjustment Result

From five different cases, we use Bundle block adjustment to solve the coordinates of check points. Case 1 will be used for reference with other cases. Case 2 and Case 3 use ground control points and manual tie points while Case 4 and Case 5 use ground control points and tie points from the computer vision method. Table 1 shows the result of 20 check points and the values of root mean square error (RMSE). The result show in Table 1. In Case 1, the RMSE in X, Y and Z direction are ±0.216 m., ±0.362 m. and ±0.308 m. respectively. In Case 2, the ground control points used only in the first and last images can reduce the RMSE inX, Y and Z direction to ±0.085 m., ±0.100 m. and ±0.039 m. respectively. In Case 3 with ground control points on all images and manual tie points the RMSE in X, Y and Z direction are respectively ±0.092 m.,±0.109 m. and±0.041 m.

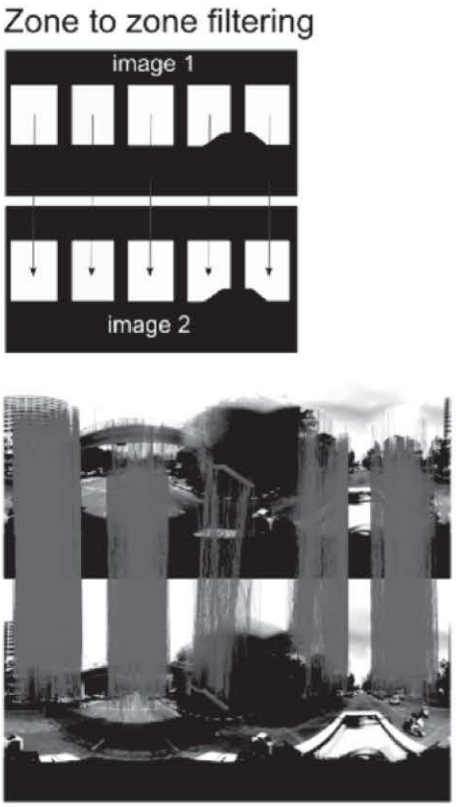

Figure 15: Zone to zone filtering result

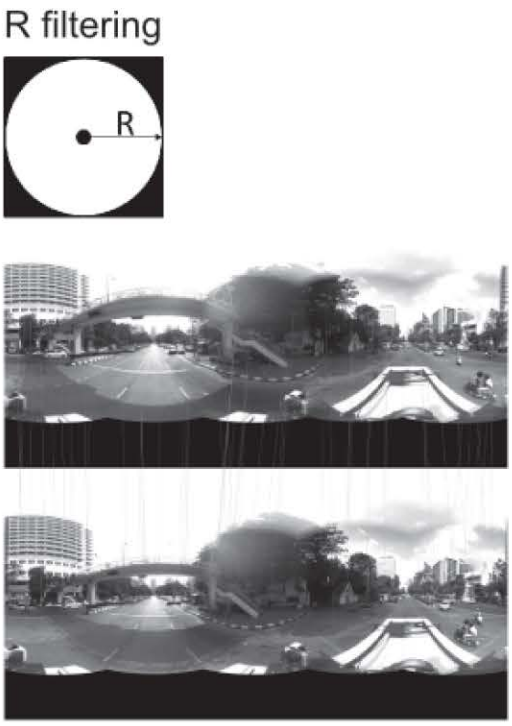

Figure 16: Radius filtering result with R= 200 pixel

Table 1: The comparing of the check points result from bundle block adjustment

Case	RMSE		
	X (m.)	Y (m.)	Z (m.)
Case 1	0.216	0.362	0.308
Case 2	0.085	0.100	0.039
Case 3	092.0	0.109	0.041
Case 4	0.303	0.330	0.202
Case 5	0.128	0.230	0.071

Table 2: The comparing of the variance result from bundle block adjustment

Case	Variance		
	X (m.)	Y (m.)	Z (m.)
Case 1	0.412	0.447	0.287
Case 2	0.191	0.207	0.133
Case 3	0.194	0.210	0.135
Case 4	0.440	0.458	0.367
Case 5	0.416	0.449	0.289

The results from these two cases do not differ significantly; as the variance results shown in Table 2 suggest, both cases remain the same. Since the exterior orientation from INS uses the main absolute location from GPS and computes with relative location from IMU, any location error will be extended to exterior orientation parameters. In contrast, the exterior orientation from bundle block adjustment with control points is more accurate. In Case 4, tie points, first found by the SURF algorithm from computer vision and then filtered to reduce mismatch, were applied to bundle block adjustment with ground control points in first and last images. The result shows the X, Y and Z direction RMSE to be ±0.303 m., ±0.330 m. and ±0.202 m. respectively. For the final case, we compute tie points from computer vision and control points on all images. The result of bundle block adjustment shows horizontal and vertical RMSE of ±0.128 m.,±0.230 m. and ±0.071 m. respectively.

The RMSE from Case 5 is less than the RMSE in Case 4 but the variance in both cases do not differ significantly (Table 2). Panoramic image matching in computer vision is still subject to error. The tie points contain mismatch points as shown by Case 4. In Case 5, the control points were used in every image and, therefore, better accuracy can be achieved. However, obtaining ground control points and tie points from computer vision has given an RMSE result that is close to that in Case 1.

5. Conclusion

In this research, a difference mathematical model is developed for spherical image from Ladybug3 as show by equation (8) and (9). This model uses bundle block adjustment. We develop a new procedure for matching interest points on images for tie points. It can eliminate a lot of mismatch point and reduce the number of points to determine the candidate tie point. This tie point will be added modify the bundle block. There search suggests that when using the exterior orientation from INS, the RMSE in X, Y and Z direction are ±0.216 m., ±0.362 m. and ±0.308 m. respectively. When the ground control points and manual tie points are used, the corresponding RMSE are ±0.085 m., ±0.100 m. and ±0.039 m. respectively. When tie points from computer vision and ground control points are used, the RMSE in X, Y and Z direction are ±0.215 m., ±0.410 m. and ±0.140 m. The RMSE decrease to±0.128 m., ±0.230 m. and ±0.071 m. in X, Y and Z direction respectively after control points are added to all images. It can be concluded that a lesser number of ground control points on first and last images can be used when location data are lost from the MMS. Our result suggests that we can apply this method to fill in gaps created by lost data in MMS work. It should also be feasible to integrate this method with panoramic image and low-cost GPS and IMU to produce low-cost MMS.

Acknowledgments

The author would like to thank Metropolitan Electricity Authority (MEA), Bangkok, Thailand for Mobile Mapping System data.

References

Bay, H., Tinne T., and Luc V. G., 2006. "Surf: Speeded up Robust Features." In Computer Vision–ECCV 2006, 404–17.

Bossler, J. D. and Toth, C., 1996, Feature Positioning Accuracy in Mobile Mapping: Results Obtained by the GPSVanTM. *International Archives of Photogrammetry and Remote Sensing*. 31 (B4): 139–42.

Edward, R. and Drummond, T., 2006, Machine Learning for High-Speed Corner Detection. *European Conference on Computer Vision*, 14.

Ellum, C. and El-Sheimy, N., 2002, Land-Based Mobile Mapping Systems. *Photogrametric Engineering and Remote Sensing*. 68 (1): 13–28.

El-Sheimy, N. and Schwarz, K. P., 1993, Kinematic Positioning in Three Dimensions using CCD Technology. *In Proceedings of the IEEE-IEE Vehicle Navigation and Information Systems Conference*, 1993, 472–75.

Fangi, G., 2007. "The Multi-Image Spherical Panoramas as a Tool for Architectural Survey." In XXI International CIPA Symposium, 1–6.

Grejner-bzezlnska, D., Toth, C. and Yudan. Y., 2005, On Improving Navigation Accuracy of GPS/INS Systems. *Photogrammetric Engineering and Remote Sensing*. 71 (4): 377–89.

Guerrero, M., 2011. "A Comparative Study of Three Image Matcing Algorithms: Sift, Surf, and Fast." Master of Science, Logan, Utah: Utah State University.

Lowe, D. G., 1999, Object Recognition from Local Scale-Invariant Features. In Computer Vision, 1999. The *Proceedings of the Seventh IEEE International Conference on*, 2:1150–57.

Muja, M. and Lowe, D., 2013, FLANN-Fast Library for Approximate Nearest Neighbors User Manual. http://www.cs.ubc.ca/research/flann/.

Novak, K. and Bossler, J. D., 1995, Development and Application of the Highway Mapping System of Ohio State University. *The Photogrammetric Record*. 15 (85): 123–34.

Tae-Wan, O. and Im-Pyeong, L., 2010, Bundle Block Adjustment of Omni-Directional Images by a Mobile Mapping System. *Korean Journal of Remote Sensing*. 26 (5): 593–603.

Santitamnont, P., 2012, Digital Photogrammetry, 2nd edition,(Chulapress). (in Thai)

Szeliski, R., 2011, Computer Vision: Algorithms and Applications. (Springer).

Uthaisri, P., Santitamnont, P. and Mityodwong, T., 2014, Comparison of Coordinates Results from MMS Exterior Orientation and Exterior Orientation from Bundle Block Adjustment. *Journal of Remote Sensing and GIS Association of Thailand*. 15 (1).(in Thai)